



UNIVERSITY OF LEEDS

This is a repository copy of *Reduced gravity processing of Cu-Co metastable monotectic alloy via drop-tube processing*.

White Rose Research Online URL for this paper:  
<http://eprints.whiterose.ac.uk/135638/>

Version: Accepted Version

---

**Proceedings Paper:**

Mullis, A [orcid.org/0000-0002-5215-9959](https://orcid.org/0000-0002-5215-9959), Jegede, O and Cochrane, R (2018) Reduced gravity processing of Cu-Co metastable monotectic alloy via drop-tube processing. In: Roosz, A, Veres, Z, Sveda, M and Karacs, G, (eds.) Proceedings of the 7th International Conference on Solidification & Gravity 2018. Solidification and Gravity 2018, 02-06 Sep 2018, Miskolc-Lillafüred, Hungary. , pp. 307-312. ISBN 978-963-508-889-8

---

This is an author produced version of a paper published in Proceedings of the 7th International Conference on Solidification & Gravity 2018.

**Reuse**

Items deposited in White Rose Research Online are protected by copyright, with all rights reserved unless indicated otherwise. They may be downloaded and/or printed for private study, or other acts as permitted by national copyright laws. The publisher or other rights holders may allow further reproduction and re-use of the full text version. This is indicated by the licence information on the White Rose Research Online record for the item.

**Takedown**

If you consider content in White Rose Research Online to be in breach of UK law, please notify us by emailing [eprints@whiterose.ac.uk](mailto:eprints@whiterose.ac.uk) including the URL of the record and the reason for the withdrawal request.



[eprints@whiterose.ac.uk](mailto:eprints@whiterose.ac.uk)  
<https://eprints.whiterose.ac.uk/>

# Reduced Gravity Processing of Cu-Co Metastable Monotectic Alloy via Drop-Tube Processing

Andrew M Mullis<sup>1</sup>, Oluwatoyin Jegede<sup>1</sup> and Robert F Cochrane<sup>1</sup>

<sup>1</sup>School of Chemical and Process Engineering, University of Leeds, Leeds LS2 9JT, UK

Corresponding author a.m.mullis@leeds.ac.uk

**Keywords:** Liquid phase separation; Core-shell structures; drop-tube processing

**Abstract.** The metastable monotectic alloy Co-Cu has been subject to rapid solidification under reduced gravity conditions via drop-tube processing, with the resulting particles being classified into 9 size fractions between 850  $\mu\text{m}$  and 38  $\mu\text{m}$ , giving cooling rates between 850  $\text{K s}^{-1}$  and 85,000  $\text{K s}^{-1}$ . Two alloy compositions were studied, Co-50 at.% Cu and Co-31.5 at.% Cu, with the undercooling required for binodal decomposition estimated as 41 K and 143 K respectively. Liquid phase separation was observed in both alloys, as were fully spherical core-shell morphologies. A statistical analysis of > 3000 particles across both compositions and all size fractions was undertaken. It was found that for both alloys the incidence of liquid phase separation increased with increasing cooling rate (decreasing particle size). For the Co-31.5 at.% Cu alloy the incidence of spherical core-shell morphologies also increased with increasing cooling rate but for the Co-50 at.% Cu alloy it was found that the incidence of spherical core-shell morphologies peaked in the 106-75  $\mu\text{m}$  size fraction, wherein  $\approx 40\%$  of all particles displayed this morphology. However, with further increases in cooling rate the incidence of core-shell structures decreased rapidly. This is thought to be due to the limited time available for migration of the two melts following liquid phase separation.

## Introduction

Monotectic alloys, such as Al-Bi and Cu-Pb, undergo liquid phase separation when cooled below a critical temperature, forming two immiscible liquids. For metastable monotectic alloys this critical temperature is below the liquidus, meaning that liquid phase separation occurs only in the undercooled melt. Examples of such systems include Ag-Ge, Al-Ag [1], Cu-Fe [2] and Cu-Co [3], among others. Many monotectic systems display a large density difference between the two liquids, making processing under terrestrial conditions problematic due to rapid buoyancy induced separation of the two liquids. However, when such materials are processed in the absence of gravity, buoyancy induced flow is eliminated and a range of unique structures can be accessed. In small droplets core-shell structures, in which a spherical core of one phase is encased in a shell of the other phase, have been observed in both stable [4] and metastable monotectic systems [5].

Such structures arise due to Marangoni convection, that is, flow driven by differences in the surface tensions of the two liquids. In the absence of buoyancy, Marangoni flow may become dominant over small length scales, wherein small temperature gradients across the cooling droplet drive the higher surface tension phase towards the core and the lower surface tension phase towards the surface of the droplet. However, the effect is far from fully understood, with not only core-shell but also three- (core-shell-corona) and even multi-layer structures being observed in some systems [5]. Moreover, some authors have claimed the core is always the lower volume fraction phase [6], while others have claimed it is always the higher melting point phase [4]. Likewise, the balance between migration velocity (increasing with increasing cooling rate) and time available for migration (decreasing with increasing cooling rate) can lead to a range of intermediate states [5] which may further complicate the analysis of such structures.

A number of novel applications have recently been suggested for monotectic alloys including: the formation under rapid cooling of amorphous-crystalline [7] or amorphous-amorphous [8] composites, the fabrication of microporous metals by selective leaching of one of the demixed

phases [9], Metal Matrix Composites (MMC's) in which the ceramic particles are confined to one of the demixed phases [10] and the formation of Cu or Ag based core-shell particles which have significant promise for electrical interconnects [4].

In this paper we investigate the metastable monotectic system Co-Cu, processed under reduced gravity conditions in the Leeds 6.5 m drop-tube. Liquid phase separation in undercooled Co-Cu alloys has previously been studied by electromagnetic levitation [3] and in both long- [11] and short- [12] drop-tubes. A range of structures have been reported including Co-rich spherulites [3],  $\alpha$ -Co dendrites at the surface of the droplet with Cu-rich spheres towards the centre [11] and uniformly dispersed Co-rich spheres in a Cu-rich matrix [12]. However, as far as we are aware, there have been no previous reports of core-shell type structures in undercooled Co-Cu melts.

## Experimental Methods

The Co-Cu master alloys for subsequent drop-tube experiments were produced by arc melting elemental Co and Cu together under a protective argon atmosphere. Two alloys were produced, with compositions of Co-50 at.% Cu and Co-31.5 at.% Cu. The equilibrium liquidus temperature for the two compositions, together with the undercooling required for binodal (nucleated) and spinodal (spontaneous) liquid phase separation to occur was determined using the CALPHAD method with the assessed thermodynamic data for the Co-Cu system given by [13].

Rapid solidification processing took place using the Leeds 6.5 m drop-tube facility. Samples of around 9 g were loaded into an alumina crucible which has three  $\times$  300  $\mu\text{m}$  holes laser drilled in the base. The crucible is loaded into a graphite sleeve which is mounted inside an induction coil at the top of the drop-tube. Processing takes place under an inert gas atmosphere at 40 kPa, with the sample being induction heated. When the desired temperature is attained, in this case a 50 K superheat above the notional liquidus temperature for the composition being processed, the crucible is pressurized to 400 kPa, wherein a spray of droplets is produced which subsequently cool and solidify in-flight down the tube. Further details of the drop-tube method are given in [14].

Once collected, the drop-tube powders are sieved into the following standard size ranges:  $> 850 \mu\text{m}$  ( $< 860 \text{ K s}^{-1}$ ), 850-500  $\mu\text{m}$  ( $860\text{-}1680 \text{ K s}^{-1}$ ), 500-300  $\mu\text{m}$  ( $1680\text{-}3300 \text{ K s}^{-1}$ ), 300-212  $\mu\text{m}$  ( $3300\text{-}5400 \text{ K s}^{-1}$ ), 212-150  $\mu\text{m}$  ( $5400\text{-}9000 \text{ K s}^{-1}$ ), 150-106  $\mu\text{m}$  ( $9000\text{-}15400 \text{ K s}^{-1}$ ), 106-75  $\mu\text{m}$  ( $15400\text{-}26700 \text{ K s}^{-1}$ ), 75-53  $\mu\text{m}$  ( $26700\text{-}47500 \text{ K s}^{-1}$ ), 53-38  $\mu\text{m}$  ( $47500\text{-}84000 \text{ K s}^{-1}$ ) and  $< 38 \mu\text{m}$  ( $> 84000 \text{ K s}^{-1}$ ). Cooling rates, which are shown in parentheses, are calculated based upon the balance of heat fluxes, using the methodology described in [14].

Some of the powders from each sieve fraction were used to confirm the bulk composition using ICP and for oxygen determination using LECO. The remainder were mounted in Transoptic resin and polished to a 1  $\mu\text{m}$  surface finish for microstructural examination, using an Olympus BX51 optical microscope and Carl Zeiss Evo MA15 Scanning Electron Microscope (SEM) which was used in backscatter detection mode. Prior to microstructural examination samples were etched in Nital solution, which preferentially dissolves the Co-rich phase thus improving contrast.

## Results

The ICP results confirm that the bulk composition of the drop-tube powders is the same as that of the starting alloy while the LECO analysis gives the oxygen content as  $< 0.02 \%$ .

The calculated phase diagram, including the metastable binode and spinode lines, as given by the CALPHAD calculation is shown in Figure 1. The critical composition is 58.7 at.% Cu, wherein liquid phase separation occurs at 1623 K, an undercooling of 13 K. For the 50.0 at.% Cu composition the liquidus, binodal and spinodal temperatures were determined as 1639 K, 1595 K ( $\Delta T = 41 \text{ K}$ ) and 1587 K ( $\Delta T = 52 \text{ K}$ ) respectively, with the corresponding values for the 31.5 at.% Cu composition being 1662 K, 1519 K ( $\Delta T = 143 \text{ K}$ ) and 1406 K ( $\Delta T = 256 \text{ K}$ ).

During microstructural analysis a range of microstructures were identified. In all but the smallest sieve fractions, the majority of droplets showed no obvious features associated with liquid phase

separation, comprising Co-rich dendrites in a Cu-rich matrix. However, in all size fractions and for both alloys, some particles could always be identified which did display characteristic signs of liquid phase separation. In some cases these were of the core-shell type, in other cases, although clear Co-rich and Cu-rich liquids had formed the migration required to form separate core and shell had either not occurred or had not gone to completion. Figure 2 shows an example of (a) a core-shell particle and (b) a liquid phase separated but non-core-shell particle. In both cases the droplets are of the Co-50.0 at.% Cu composition, with that shown in part (a) being from the 150 – 212  $\mu\text{m}$  size fraction while that shown in part (b) is from the 75 – 106  $\mu\text{m}$  size fraction. Both micrographs are taken using backscatter imaging, wherein the Co-rich phase appears dark and the Cu-rich phase light. In the case of the non-core-shell particle shown in Figure 2b there is clear evidence that the Co-rich region is evolving towards spherical and we believe that this particular morphology arose due to freezing of the droplet prior to spheroidisation of the core going to completion.

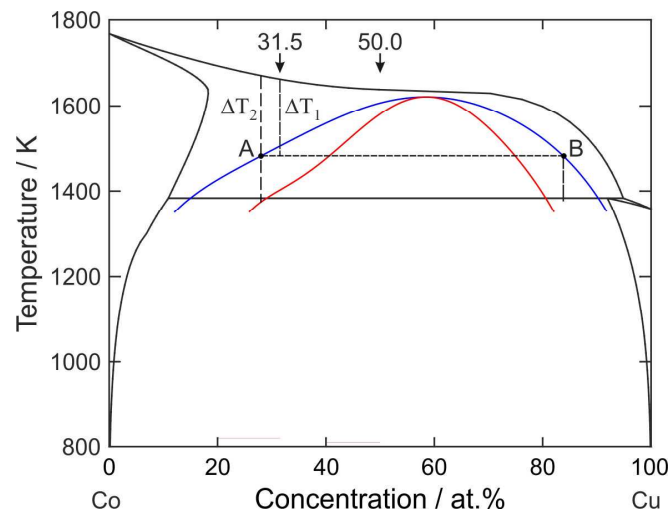


**Figure 1.** Phase diagram for the Co-Cu system showing the metastable binode (blue) and spinode (red). Also shown are the compositions of the two alloys considered in this work. Points ‘A’ and ‘B’ show the compositions of the Co- and Cu-rich liquids formed by binodal decomposition at an undercooling  $\Delta T_1$ . Due to the asymmetry of the phase diagram, further undercooling to  $\Delta T_2$  would result in secondary (spinodal) decomposition of the Co-rich, but not the Cu-rich, liquid.

One feature to note that is common to both microstructures shown in Figure 2, is the fine dispersion of Cu-rich particles and filaments in the bulk Co-rich region. The very fine nature of this dispersion, together with its interconnected filament like nature, leads us to believe this arises due to spinodal decomposition and is indicative of both samples shown in Figure 2 of having undergone two episodes of liquid phase separation, binodal, followed by spinodal. Interestingly, where we observe such instances of double decomposition, we always observe a fine dispersion of Cu-rich filaments in the bulk Co-rich region but only sometimes do we observe the corresponding fine dispersion of Co-rich filaments in the bulk Cu-rich region. Figure 2a shows both, but in Figure 2b the fine filament type dispersion is much less widespread in the bulk Cu-rich regions than in the bulk Co-rich region. We believe this arises due to the asymmetry in the binode and spinode lines.

The basic mechanism is illustrated on Figure 1, for an alloy at 31.5 at.% Cu, although the process would also work for the 50.0 at.% Cu composition. Due to rapid cooling, and the division of the melt into small droplets, the melt will undercool in-flight. As the binodal decomposition is a nucleated transition the first episode of liquid phase separation will not necessarily occur at the binodal temperature, but at some point below this, let us assume at an undercooling  $\Delta T_1$ . Binodal decomposition will result in the formation of Co- and Cu-rich liquids, the composition of which is given by the binode line of the metastable phase diagram. These points are labelled ‘A’ and ‘B’

respectively on Figure 1. With further cooling the total undercooling could now reach a level  $\Delta T_2$ , wherein the Co-rich liquid will reach the spinodal decomposition temperature, with a second episode of spontaneous liquid phase separation occurring. However, due to the asymmetry in the phase diagram the Cu-rich liquid will still be substantially above its spinodal decomposition temperature, wherein secondary decomposition may occur in one phase only, or with sufficient undercooling, both phases.

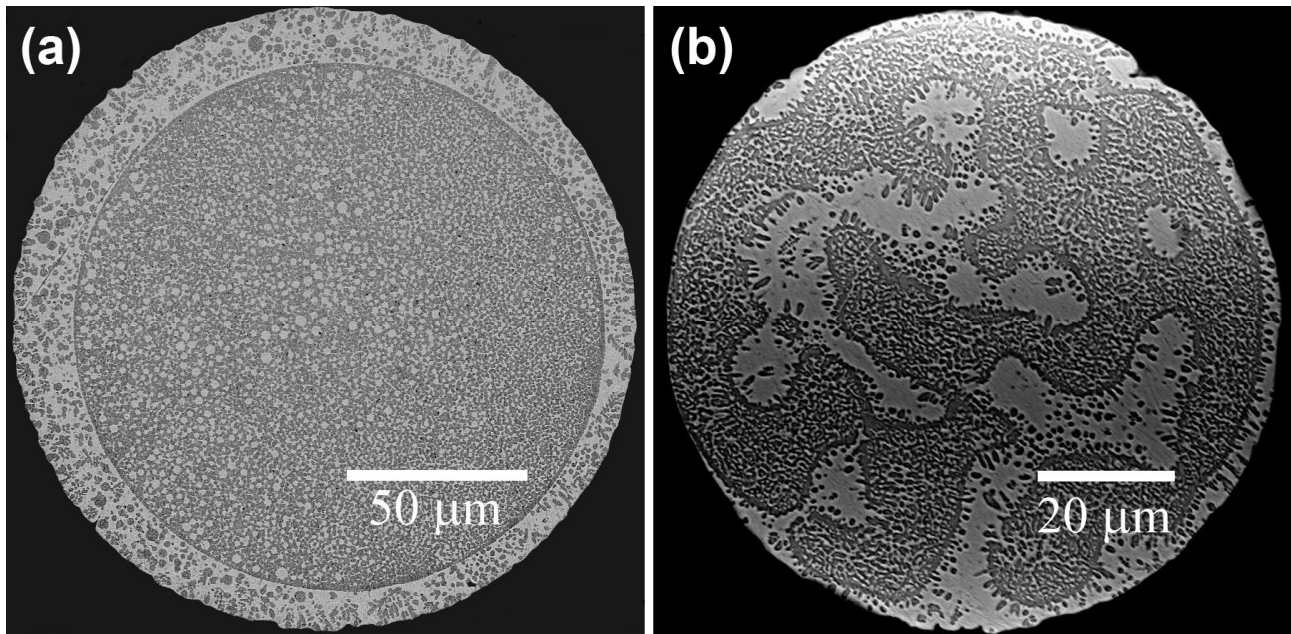


**Figure 2.** Two liquid phase separated droplets from the Co-50 at.% Cu alloy: (a) displaying a well-developed core-shell structure and clear evidence of secondary (spinodal) liquid phase separation in both the Co-rich and Cu-rich phases and (b) a droplet frozen before full agglomeration of the Co-rich phase to form the core. Note that secondary liquid phase separation is clearly evident in the bulk Co-rich (dark) phase but much less so in the bulk Cu-rich phase.

The stochastic nature of nucleation, both for binodal decomposition and ultimately for solidification, mean that we observe a range of microstructures in all particle size fractions. The prevalence of liquid phase separation as a function of droplet size is shown in Figure 3a for both the 50.0 at.% and 31.5 at.% Cu alloys. The data contained in the figure is based on a microstructural classification of > 1500 particles for each composition, with not less than 100 particles in any size fraction. The general trend is for the proportion of such droplets to increase with decreasing droplet size, which is as expected as high cooling rates favour deep undercooling as does the lower number of potential heterogeneous nucleation sites in the smaller droplets. Moreover, the higher undercooling required to access liquid phase separation in the 31.5 at.% Cu alloy means that the prevalence of such droplets is lower in this alloy. Figure 3b shows, as a proportion of the total number of droplets, the prevalence of particles containing a fully spherical core, as a function of droplet size, wherein a more complex trend is apparent. For the 50 at.% Cu alloy, the incidence of core-shell structures peaks in the 75–106  $\mu\text{m}$  sieve fraction before decreasing sharply for yet smaller particles, despite the increasing incidence of liquid phase separation. This observation can be understood as, at the higher cooling rates, although the undercooling of the melt increases the time available for migration of the Co-rich melt to the core prior to solidification, decreases. Consequently, the incidence of fully spherical core-shell particles decreases. These are replaced by structures which display liquid phase separation, but have not undergone complete core-shell migration, such as that shown in Figure 2b. The main difference between the two compositions is

apparent in Figure 3b. Specifically, the incidence of fully spherical core-shell particles continues to increase with increasing cooling rate in the Co-rich composition, rather than peaking at some intermediate undercooling, as is the case for the 50-50 (at.%) composition. This may reflect the larger core requiring less time to form as there will be significantly more Co-rich material available following liquid phase separation in the 31.5 at.% Cu alloy.

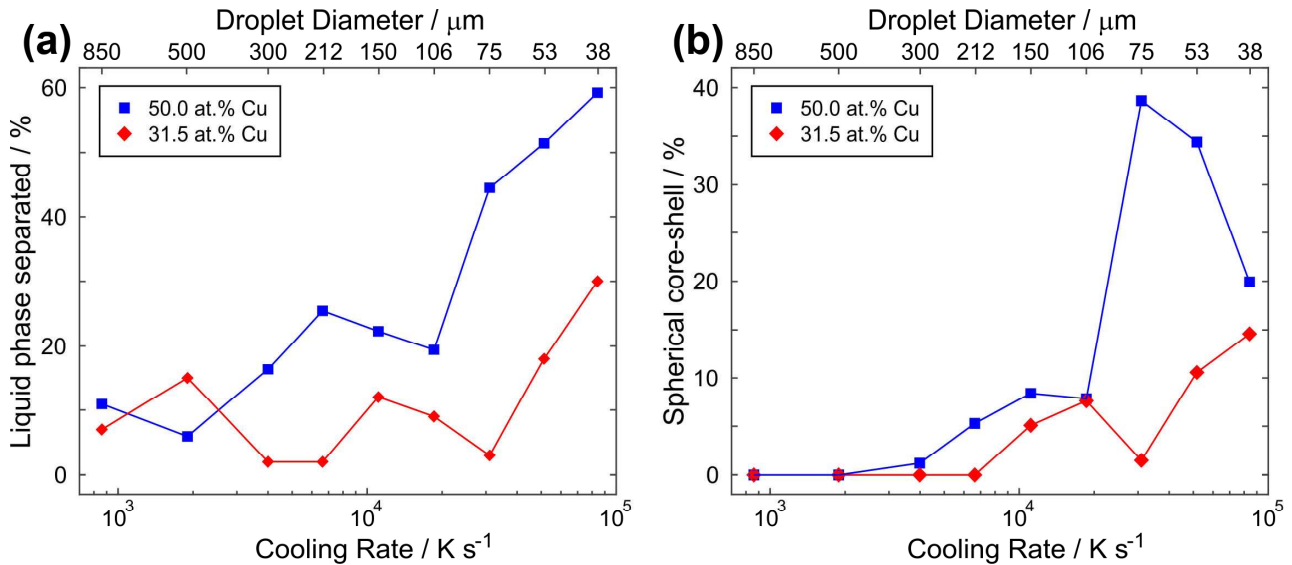


**Figure 3.** (a) Fraction of droplets, for both compositions, that are observed to undergo liquid phase separation as a function of cooling rate (droplet size) and (b) the fraction of droplets that form fully spherical cores, again as a function of cooling rate (droplet size) and for both compositions.

## Summary

Liquid phase separation has been studied in the metastable monotectic Co-Cu system. Contrary to previous work on this system we find clear evidence for the formation of core-shell structures. A statistical analysis of the prevalence of liquid phase separation and of the formation of core-shell structures has been undertaken. We find that in the 31.5 at.% Co alloy studied, liquid phase separation and core-shell structures are both most prevalent at the highest cooling rates achieved. In contrast, in the 50.0 at.% Cu, although liquid phase separation is still most common at the highest cooling rates, core-shell formation peaks at intermediate cooling rates. This is thought to reflect the time available for migration of the two separated liquids into the core and shell regions.

## References

- [1] L. Ratke, G. Korekt, S. Brück, F. Schmidt-Hohagen, G. Kasperovich, M. Köhler, Phase equilibria and phase separation processes in immiscible alloys, in: 2nd Sino - Ger. Symp. (2009).
- [2] N. Liu, Investigation on the phase separation in undercooled Cu-Fe melts, *J. Non. Cryst. Solids.* 358 (2012) 196–199.
- [3] A. Munitz, R. Abbaschian, Microstructure of Cu-Co Alloys Solidified at Various Supercoolings, *Metall. Mater. Trans. A.* 27 (1996) 4049–4059.
- [4] R. Dai, S.G. Zhang, Y.B. Li, X. Guo, J.G. Li, Phase separation and formation of core-type microstructure of Al-65.5 mass% Bi immiscible alloys, *J. Alloys Compd.* 509 (2011) 2289–2293.
- [5] C.P. Wang, X.J. Liu, I. Ohnuma, R. Kainuma, K. Ishida, Formation of immiscible alloy powders with egg-type microstructure, *Science* 297 (2002) 990–993

- [6] R.P. Shi, C.P. Wang, D. Wheeler, X.J. Liu, Y. Wang, Formation mechanisms of self-organized core/shell and core/shell/corona microstructures in liquid droplets of immiscible alloys, *Acta Mater.* 61 (2013) 1229–1243.
- [7] J. He, H. Jiang, S. Chen, J. Zhao, L. Zhao., Liquid phase separation in immiscible Ag–Ni–Nb alloy and formation of crystalline/amorphous composite *J. Non-crystalline Solids* 357 (2011) 3561–3564.
- [8] A Concustell, N Mattern, H Wendrock, U. Kuehn, A. Gebert, J. Eckert, A.L. Greer, J. Sortd, M.D. Baro, Mechanical properties of a two-phase amorphous Ni–Nb–Y alloy studied by nanoindentation, *Scripta Mater.* 56 (2007) 85–88.
- [9] H Yasuda, I Ohnaka, S Fujimoto, N. Takezawa, A. Tsuchiyama, T. Nakano, K. Uesugi, Fabrication of aligned pores in aluminum by electrochemical dissolution of monotectic alloys solidified under a magnetic field, *Scripta Mater.* 54 (2006) 527–532.
- [10] I Budai & G Kaptay, Wettability of SiC and alumina particles by liquid Bi under liquid Al, *J. Mater. Sci.* 45 (2010) 2090–2098.
- [11] X. Luo, L. Chen, Investigation of microgravity effect on solidification of medium-low-melting-point alloy by drop tube experiment, *Sci. China Ser. E Technol. Sci.* 51 (2008) 1370–1379.
- [12] C. Cao, N. Wang, B. Wei, Containerless rapid solidification of undercooled Cu-Co peritectic alloys, *Sci. China Ser. A Math.* 43 (2000) 1318–1326.
- [13] T Nishizawa, K Ishida, The Co-Cu (Cobalt-Copper) system, *Bull. Alloy Phase Diagrams*, 5 (1984) 161–165.
- [14] O.R. Oloyede, T.D. Bigg, R.F. Cochrane, A.M. Mullis, Microstructure evolution and mechanical properties of drop-tube processed, rapidly solidified grey cast iron, *Mater. Sci. Eng. A*, 654 (2016) 143–150.